communications earth & environment

Article

A Nature Portfolio journal

https://doi.org/10.1038/s43247-025-03058-7

Carbon dynamics control contemporary mercury burial in Arctic Ocean sediments

Charles Gobeil [1] ✉, Sophia C. Johannessen [2], Miguel A. Goñi[3], Zou Zou A. Kuzyk[4] & Daniel Cossa[5]

Understanding the high mercury concentrations observed in Arctic ecosystems requires in-depth knowledge of mercury cycling. Here, we show that variations in mercury concentration in the sediments of the North American Arctic Margin and the Arctic Ocean basins can be explained by carbon sources and cycling. Sedimentary mercury concentrations are predicted ($p < 0.001$) considering three carbon sources and, in some areas, the recapture of soluble mercury released during burial. Terrigenous organic carbon dominates mercury delivery (50-90%) in the western North American Arctic Margin, whereas inorganic carbon predominates at many eastern sites (40-70%). Marine organic carbon contributes <15% of the total mercury concentration. Mercury–organic carbon endmember ratios of terrigenous and marine organic carbon are higher in deep Arctic Ocean basins than in the continental margin, likely due to greater organic matter remineralization during transit. The observed enrichment in mercury toward the sediment surface results from remineralization of organic carbon, not from an increase in mercury flux.

Mercury (Hg) is of persistent concern in the Arctic Ocean (AO), because higher-trophic level Arctic marine organisms contain elevated concentrations of this bioaccumulative, neurotoxic element[1–3]. Hg arrives in the AO from both natural and anthropogenic sources. It follows complex pathways through the marine environment, and a portion of the Hg is buried in sediments, where it is eventually isolated from the pelagic food web. Despite multiple research initiatives, the modern Hg cycle in the AO nevertheless remains ill-defined, particularly as regards i) its processing and burial in bottom sediments and ii) the imprint that long-range atmospheric and oceanic transport of anthropogenic Hg might have on this cycle[4–6]. There is a widespread pattern of increasing Hg concentration toward the surface of AO sediments[6–10], but it has been unclear whether this trend emerges from an increase in the flux of Hg into the ocean or as a result of diagenetic mechanisms within the sediment.

Furthermore, Hg is thought to be transferred to AO sediments mainly in association with settling particles of marine (*autochthonous*) organic carbon (OC_{MAR})[4,5], as is the case in other oceans[11–16]. However, terrigenous (*allochthonous*) organic carbon (OC_{TERR}) predominates in marginal and deep basin sediments of the AO[17,18], and Hg that enters the AO from continental sources is largely bound to OC_{TERR}[19–23]. In addition, even though inorganic carbon (IC) is abundant in certain Arctic marine regions, such as areas in the Canadian eastern Arctic[24,25], the role of IC in Arctic Hg cycling has not been examined.

Here, we investigate what controls Hg surface enrichment in Arctic Ocean sediments, including the roles of carbon sources and organic carbon (OC) remineralization in the water column and sediments. We use a set of 24 sediment box-cores that spans a range of productivity and terrigenous flux across the North American Arctic Margin (NAAM), applying carbon isotopes ($\delta^{13}C$) to differentiate marine and terrigenous organic carbon, together with six basin cores previously analyzed for Hg and other elements[10] (Fig. 1 and Supplementary Table 1).

Results and discussion

Regional and vertical variability of Hg and OC

The Hg and OC concentrations vary spatially and with depth in sediments across the NAAM (Fig. 2 and Supplementary Table 2 and Data 1). The Hg concentrations in the 24 cores analyzed range from 2 to 98 ng g^{-1} and those of OC from 1 to 26 mg g^{-1}. Hg remains relatively invariant or slightly decreases with depth in cores CAA1, CAA2 and UTN7, but in all the other 21 NAAM cores it decreases with depth below the sediment–water interface (Fig. 2), as also observed for OC. The most substantial declines occur in the uppermost 10 cm, which represents an average of 106 ± 42 years of sediment accumulation[26]. The Hg:OC ratio varies little (13 ± 9%) and exhibits no systematic trend with depth in the cores, except in five of the Bering and Chukchi Seas cores, where it increases slightly but steadily between the sediment surface and 5–10 cm depth (Supplementary Fig. 1). In contrast to

[1]Institut national de la recherche scientifique, Université du Québec, Québec, QC, Canada. [2]Department of Fisheries and Oceans, Institute of Ocean Sciences, Sidney, BC, Canada. [3]College of Earth, Ocean and Atmospheric Sciences, Oregon State University, Corvallis, OR, USA. [4]Center for Earth Observations Science, University of Manitoba, Winnipeg, MB, Canada. [5]Institut des sciences de la terre, Université Grenoble Alpes, Grenoble, France. ✉e-mail: charles.gobeil@inrs.ca

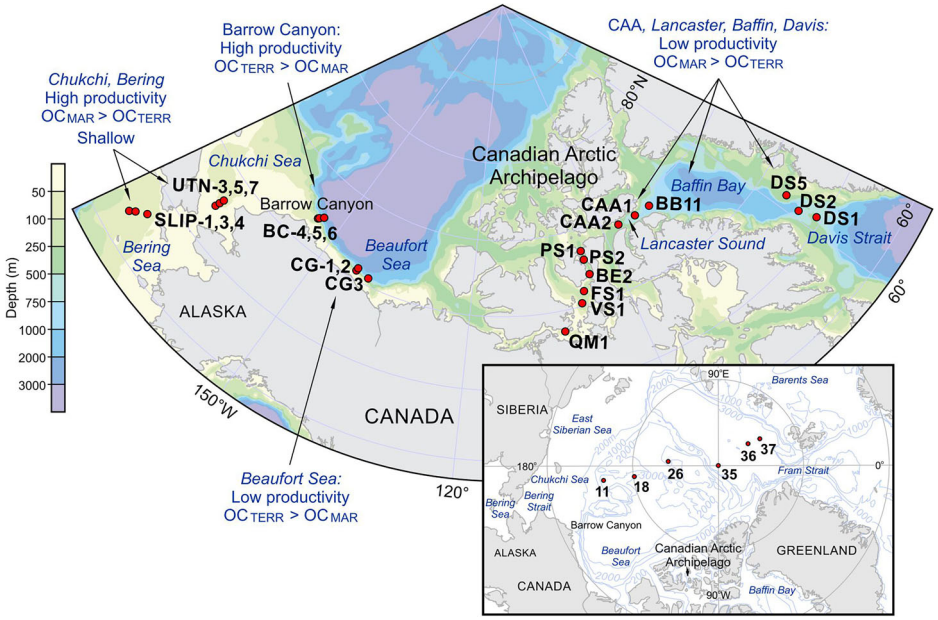

Fig. 1 | Map of the North American Arctic Margin showing the coring sites, areas of high and low productivity, and the relative concentrations of marine (MAR) and terrigenous (TERR) organic carbon (OC) in the sediments of different regions. Inset: locations of the sediment cores from the deep central Arctic Ocean previously analyzed for mercury (Hg)[10].

Hg and OC, reduced sulphur (i.e., acid volatile sulphide + chromium reducible sulphur) is low in surface sediment and increases with depth (Supplementary Fig. 2), indicating sulphate reduction under anoxic conditions[27]. Cores with smaller inventories of reduced sulphur (e.g., the Canadian Archipelago cores) tend to have well-defined surface enrichments of Fe oxyhydroxides (Supplementary Fig. 3), which are indicative of anaerobic organic matter oxidation by ferric iron-reducing bacteria[27]. In the cores from the Bering and Chukchi Seas that are characterized by the most elevated reduced sulphur inventories, the absence of such Fe surface enrichments testifies to the very limited O_2 penetration depth (< 0.5 cm) in the sediments[28,29].

Moreover, while Hg covaries positively ($p < 0.001$) with OC, the slope of the linear regression varies regionally (Fig. 3). In the NAAM, the shallowest slope (lowest Hg:OC ratio) is observed in the Bering and Chukchi Seas (1.2 $\mu g_{Hg}\ g_{OC}^{-1}$), while the steepest slope (5.3 $\mu g_{Hg}\ g_{OC}^{-1}$) is found in the Beaufort Sea (cores CG2 and CG3). Steeper slopes (9.5 $\mu g_{Hg}\ g_{OC}^{-1}$) have been previously calculated for sediments collected at water depths of 2265–4230 m in the Amerasian and Eurasian Basins of the central AO[10] (Fig. 3 and Supplementary Data 2). Although all the regional linear relationships between Hg and OC have non-zero y-intercepts (i.e., for OC = 0 mg g^{-1}), these values are close to or not statistically different from zero ($p < 0.01$), with the exception of that characterizing the sediments of the Bering and Chukchi Seas (see Fig. 3 and Supplementary Table 3).

Relationship between the Hg:OC ratio and carbon isotope composition of OC

The stable isotope composition of OC ($\delta^{13}C$) was determined in samples from all the cores, except Lancaster Sound core CAA2. Overall, the $\delta^{13}C$ values range from –25.2‰ to –20.1‰, with the lowest values in Beaufort Sea (–24.2 ± 0.3‰, $n = 18$) and Barrow Canyon (–23.5 ± 0.8 ‰, $n = 51$), and higher values in Lancaster Sound (–22.0 ± 0.2 ‰, $n = 42$), the Canadian Archipelago (–21.5 ± 0.5 ‰, $n = 43$), the Chukchi and Bering Seas (–21.5 ± 0.4‰, $n = 36$), and Davis Strait (–20.7 ± 0.7‰, $n = 16$). Without considering the results for the five cores from the interior of the Canadian Archipelago (VS1, FS1, BE2, PS2 and PS1), in which IC concentrations are particularly elevated (30–60 mg g^{-1}; Supplementary Fig. 4), the Hg:OC ratios in NAAM sediments are negatively correlated ($p < 0.001$) with increasing $\delta^{13}C$ values (Supplementary Fig. 5). In the IC-enriched Canadian Archipelago cores, however, Hg:OC ratios do not follow the same trend; they are higher than those of sediments from other regions (Lancaster Sound, Davis Strait, Bering and Chukchi Seas) having similar $\delta^{13}C$ values (Supplementary Fig. 5).

Diagenetic control of sedimentary Hg profiles

The linearity of the regional Hg–OC relationships in NAAM sediments, and the fact that Hg concentrations tend to zero as OC concentrations also approach zero, show that particulate OC is the major Hg-binding phase. Furthermore, the stability of the Hg:OC ratio with depth in most cores indicates that the Hg profiles are not determined by a modification in Hg flux, but by OC dynamics within the sediment. If the Hg enrichment in surface sediment were the result of increasing anthropogenic flux, the Hg:OC ratio would also be higher toward the surface, which is not the case. If the anthropogenic flux had coincidentally increased at exactly the same rate as an increase in organic carbon (perhaps as a consequence of the thawing of permafrost), that could also result in a constant Hg:OC ratio, but only over a restricted timeframe. Our data show nearly invariant Hg:OC ratios over the full length (≤45 cm) of most cores. Based on the geochronology presented by Kuzyk et al.[29], 45 cm in these cores represents up to 475 years of sedimentation. In contrast, anthropogenic Hg contamination was likely not substantial in the Arctic Ocean before the late 1800s[30]. Consequently, we conclude that the trends in these cores represent diagenetic effects, not increasing Hg flux.

The stable Hg:OC ratio with depth in most cores implies that Hg released during early OC oxidation does not precipitate or form solid-phase complexes, either with organic matter or with authigenic oxyhydroxide or sulphide minerals[31–35]. If that were the case, the Hg:OC ratio would decrease or increase with depth in the sediments, depending on whether Hg reacted with oxyhydroxides or sulphides[36], because the total amount of Hg would remain the same, while the OC declined with depth. Rather, our results imply that Hg is mobilized from the solid phase as a consequence of OC metabolism in the benthic boundary layer and lost from the sediments. As argued in other works[37,38], a plausible mechanism might be that Hg migrates out of the sediments following its methylation by sulphate– and ferric iron–reducing bacteria and the subsequent transformation of the resulting monomethylmercury into volatile Hg species (Hg^0, $Hg(CH_3)_2$)[39–41]. Although our dataset does not confirm that these reactions occur in AO sediments, the vertical profiles of Fe oxyhydroxides and reduced sulphur in the cores (Supplementary Figs. 2 and 3) testify that the redox conditions are fulfilled. We conclude that the Hg decline with depth in the cores is due to post-depositional release and benthic diffusion of elemental or methylated

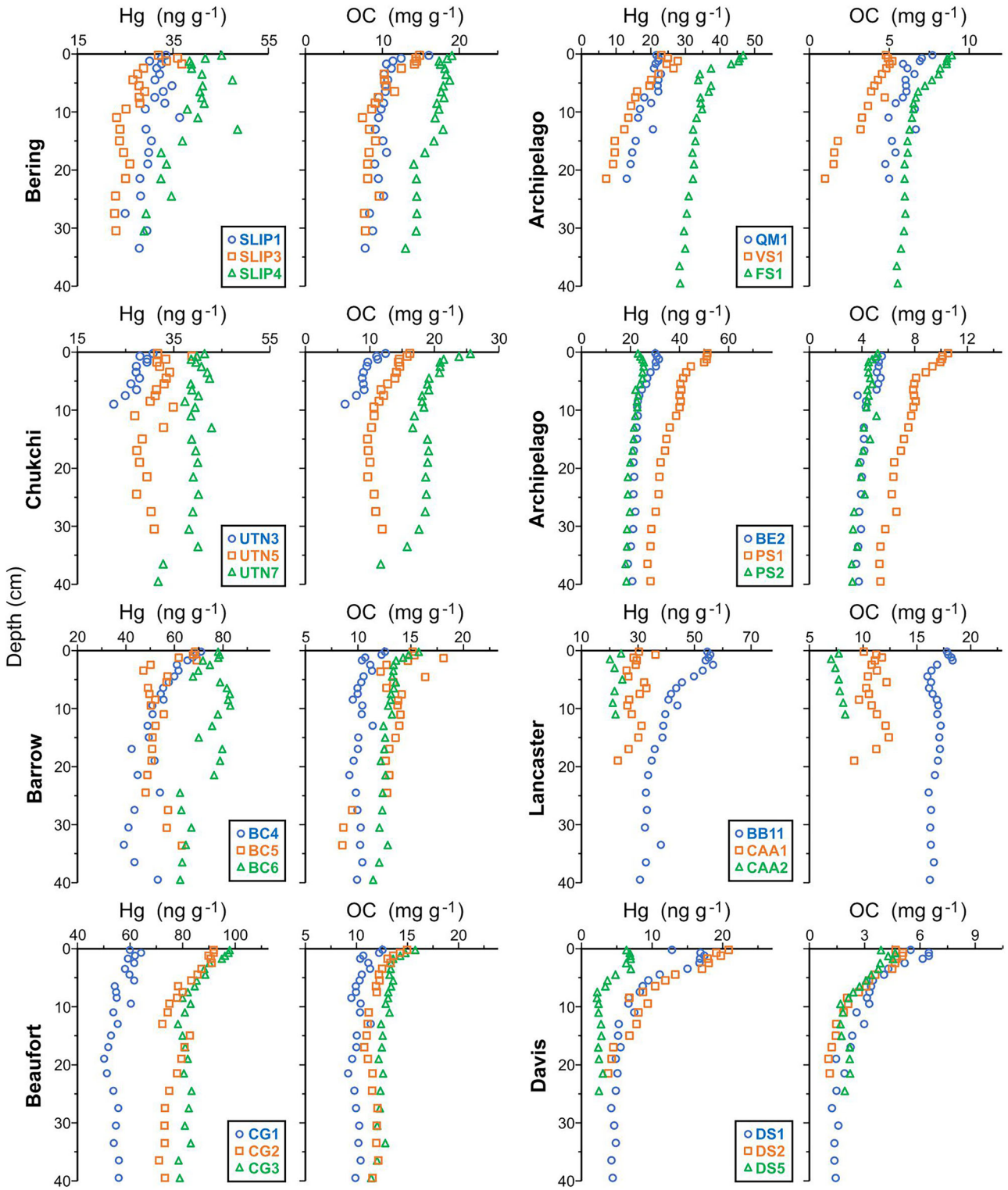

Fig. 2 | Sediment core profiles of mercury (Hg) and organic carbon (OC), grouped by region. Note that the concentration scales vary among plots to better illustrate the shapes of the profiles. Cores from the same region in each of the plots are distinguished with colours and symbols.

Hg produced as OC is oxidized in the suboxic zone of the sediment. This conclusion is supported by recent field data showing that the methylmercury input from shelf sediments in the Arctic Ocean could be as much as twice that of river discharges[42].

The only exception to this inference is for the cores from the Bering and Chukchi Seas, where the Hg:OC ratio increases with core depth over the top 5–10 cm of sediment (Supplementary Fig. 1). These marine areas are characterized by high primary productivity and a shallow water column (Fig. 1), meaning that a high flux of labile OC reaches the sediment[28]. The oxygenated sediment surface layer at these sites is consequently shallow (<0.5 cm), and there is a relatively high reduced sulphur concentration near the sediment surface (Supplementary Fig. 2)[28,29]. These observations suggest that, as Hg is released from its association with labile OC, it is captured through surface complexation reactions with iron sulphide minerals or as a

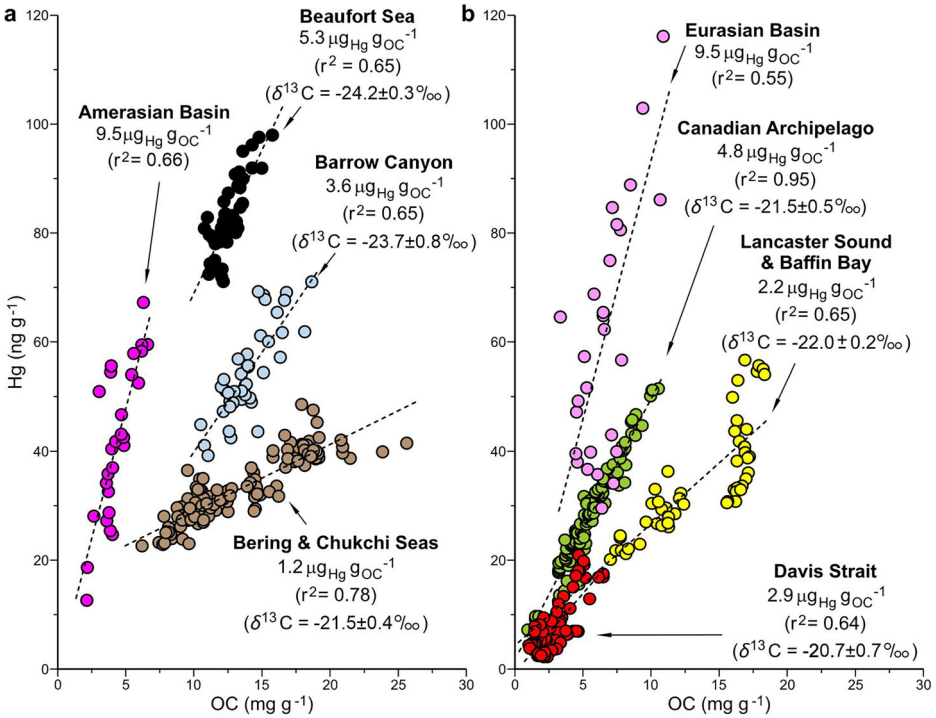

Fig. 3 | Relationship between mercury (Hg) and organic carbon (OC) in sediment of the North American Arctic Margin (NAAM) and central Arctic Ocean basins. Results for the western NAAM and Amerasian Basin are shown in (**a**) and those for the eastern NAAM and Eurasian basin in (**b**). The slope (Hg:OC ratio) is marked for each region, along with the average stable isotope composition of OC ($\delta^{13}C$) for the region, which was used to determine the proportion of terrigenous material. Regression lines are all highly significant ($p < 0.001$). The 99% confidence intervals on the slope of the linear fits of the data and the y-intercept are reported in Supplementary Table 3. Values for different regions are characterized by distinctive colours.

precipitate of HgS[31,32]. This pattern is not observed at other NAAM sites, where the OC is less labile, O_2 is less rapidly consumed, and reduced sulphur is not produced so close to the sediment surface.

Role of carbon source composition in sedimentary Hg concentrations

The trend of decreasing Hg:OC ratio with increasing $\delta^{13}C$ values in NAAM sediments (Supplementary Fig. 5) indicates that the relative proportions of marine and terrigenous OC are likely the major causal factor for the regional differences in the Hg:OC ratio. Assuming previously-identified $\delta^{13}C$ endmember values for OC_{TERR} (–26.5‰) and OC_{MAR} (–19.5‰) in our study area[24,43–45], it can be seen that sediments with the highest OC_{TERR} content have higher Hg:OC ratios (Fig. 3). The significant, positive intercepts (16.5 ± 2.3 ng g^{-1}) of the Hg–OC relationship observed in the sediments of the Bering and Chukchi Seas (Supplementary Table 3) likely result from the presence of a Hg fraction associated with inorganic material, including reduced sulphur, as discussed above, but also carbonate and aluminosilicate minerals.

Previous studies have reported Hg concentrations in a variety of sedimentary calcareous rock samples (see Methods). Here we have considered a value of 42 ± 12 ng g^{-1}, which corresponds to the average ± one standard error (hereafter identified as SE) of the Hg concentration reported for Paleozoic shales widely distributed across the eastern seaboard of Canada[46], and is within the range of values characterizing a variety of calcareous sedimentary rocks (4-220 ng g^{-1})[47]. From this value a Hg:IC endmember ratio of 0.35 ± 0.05 $\mu g_{Hg}\ g_{IC}^{-1}$ can be derived (see Methods). Presuming that carbonate minerals (calcite and dolomite) from detrital sources accumulating in NAAM sediments[24,25] are characterized by a similar endmember Hg:IC ratio, the supply of Hg to the sediments from this material (Hg_{IC}) can be assessed on the basis of the IC concentrations. As illustrated in Supplementary Fig. 6, this contribution would be very low (<1 $ng_{Hg}\ g_{SED}^{-1}$) in the Bering and Chukchi Seas and moderate (1–7 $ng_{Hg}\ g_{SED}^{-1}$) in the Barrow Canyon and Beaufort Sea. In the interior of the Canadian Archipelago, the contributions of Hg from the IC source could be as high as 12–19 $ng_{Hg}\ g_{SED}^{-1}$, thus representing approximately 40–70% of the Hg concentration at many locations.

Mercury from aluminosilicate rocks also contributes to the Hg content of NAAM sediments, but its contribution is relatively small. Considering the aluminium (Al) concentrations in our sediment samples (Supplementary Data 2) and a Hg:Al ratio of 30 ± 6 (SE) $ng_{Hg}\ g_{Al}^{-1}$ [48] (see Methods), the Hg contribution from aluminosilicates (Hg_{Al}) in NAAM sediments is estimated to be on the order of 1.7 ± 0.1 (SE) $ng_{Hg}\ g_{SED}^{-1}$.

To quantify the contributions of Hg from OC_{MAR} and OC_{TERR} sources to NAAM sediments, we need to estimate their Hg:OC endmember ratios (see Methods). The fraction of OC from a terrigenous source (F_{TERR}) and the concentrations of OC_{MAR} and OC_{TERR} were determined using a simple, two-source mixing model, with measured concentrations and isotopic compositions of OC and previously-reported $\delta^{13}C$ endmember values for OC_{TERR} (–26.5‰) and OC_{MAR} (–19.5‰)[24,43–45]. The Hg:OC ratio free of inorganic Hg was determined as follows. For all samples, except for those from the Bering and Chukchi Seas, inorganic Hg is assumed to be exclusively attached to IC (Hg_{IC}) and aluminosilicates (Hg_{Al}). However, for the Bering and Chukchi Seas sediments, inorganic Hg also includes a component from sulphide minerals that can be estimated from the positive intercept at OC = 0 of the Hg—OC relationship (see Methods). The Hg:OC endmember ratios (± 99% confidence interval) for OC_{MAR} and OC_{TERR} were then obtained, using the y-intercepts of the regression line of Hg:OC vs. F_{TERR} at $F_{TERR} = 0$ (0.39 ± 0.40 $\mu g_{Hg}\ g_{OCMAR}^{-1}$) and $F_{TERR} = 1$ (6.3 ± 0.9 $\mu g_{Hg}\ g_{OCTERR}^{-1}$), respectively (Fig. 4a). Multiplying these values by the OC_{MAR} and OC_{TERR} concentrations, respectively, indicates that OC_{TERR} dominates Hg delivery (50-90%) to western NAAM sediments and is also a key Hg carrier (20-80%) on the eastern side of the margin (Supplementary Fig. 6). OC_{MAR} never represents more than 15% of the measured Hg concentrations. Note that, although the uncertainty on the Hg:OC_{MAR} endmember is relatively high, its value is more than 10 times lower than the Hg:OC_{TERR} endmember ratio, so we are confident that our approach can quantitatively distinguish the two types of organic matter sources.

The comparison between measured Hg concentrations and modelled concentrations (Fig. 4b), the latter being defined as the cumulative concentrations of Hg associated with OC_{MAR}, OC_{TERR}, IC, aluminosilicates and sulfide minerals, confirms that: (i) our measurements are internally consistent, (ii) the endmember values for the different Hg sources are well characterized, and (iii) we have accounted for all major sources of Hg. These

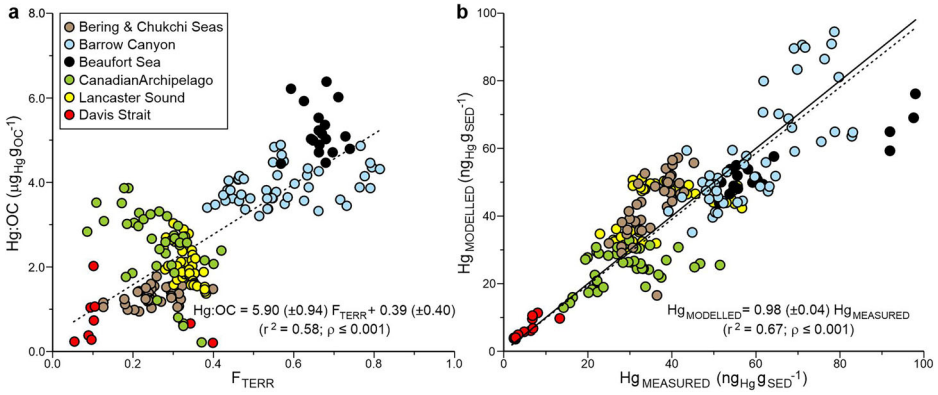

Fig. 4 | Relationships between the mercury–organic carbon ratio (Hg:OC) and the fraction of terrigenous OC (F_{TERR}), and between the modelled and measured Hg concentrations in North American Arctic Margin sediments. In (**a**), the Hg:OC ratio was determined after having subtracted the estimated concentration of Hg associated with carbonates, aluminosilicates and sulphide minerals from the measured Hg concentration. In (**b**), $Hg_{MEASURED}$ and $Hg_{MODELLED}$ correspond to measured and modelled Hg concentrations, respectively. The uncertainties on the slope and y-intercept of the linear fit in both panels represent the 99% confidence intervals. The solid black line in (**b**) illustrates an ideal 1:1 relationship between $Hg_{MODELLED}$ and $Hg_{MEASURED}$. Values for different regions are characterized by distinctive colours.

findings imply that other potential sources are small relative to those identified. The predictive power of the mixing model convincingly demonstrates that carbon composition is the most important factor determining the Hg content of AO sediments. Further, a single set of endmembers is sufficient to characterize the variability in Hg concentrations across the whole NAAM. The $Hg:OC_{TERR}$ ratio (6.3 ± 0.9 $\mu g_{Hg}\ g_{OCTERR}^{-1}$) is at least an order of magnitude higher than the $Hg:OC_{MAR}$ (0.39 ± 0.40 $\mu g_{Hg}\ g_{MAR}^{-1}$) and Hg:IC (0.35 ± 6 $\mu g_{Hg}\ g_{IC}^{-1}$) ratios. Since the concentrations of OC_{TERR} are much higher than those of OC_{MAR} and IC in the western NAAM sediments, these ratios imply that OC_{TERR} is the main Hg carbon source in that area. However, due to the strong carbonate enrichment of the Canadian Arctic Archipelago sediments, IC also represents an important Hg contributor at many eastern NAAM sites.

There are fewer data available from which to test the mixing model in the deep Arctic basins. However, it is possible to infer sedimentary $Hg:OC_{TERR}$ and $Hg:OC_{MAR}$ endmembers at our deep basin coring sites (see Methods), using the following assumptions: (i) Hg associated to reduced sulphur is negligible, (ii) the Hg:IC and Hg:Al endmember values calculated for the NAAM also apply to basin sediments, and (iii) OC_{TERR} represents 80% of the total sedimentary OC content in the central AO sediments[17,49]. At these locations, the best fit between the measured and simulated Hg concentrations is obtained with terrigenous and marine endmembers of 11.2 $\mu g_{Hg}\ g_{OCTERR}^{-1}$ and 0.80 $\mu g_{Hg}\ g_{OCMAR}^{-1}$, respectively (Supplementary Fig. 7). Both of these Hg:OC endmembers for the deep basins are substantially higher than at the shallower sites. Although some OC likely continues to be degraded in basin sediments, the measured Hg:OC ratios in the basin cores, like those in the NAAM, are approximately constant with depth. This implies that the higher Hg:OC ratios in the basin relative to the NAAM probably do not result from higher OC degradation within these slowly-accumulating sediments. Rather, the higher ratios likely relate to the greater horizontal and vertical distances that a particle has to travel to reach the deep basin, which result in greater OC remineralization in the water column, as discussed below.

Role of OC remineralization on sedimentary Hg concentrations

The isotopic signature of Hg in Arctic Ocean sediments shows that Hg is mainly from terrigenous sources, primarily permafrost[6]. However, it appears that the sedimentary Hg:OC ratio is much higher than that of permafrost. Lim et al.[50] have reviewed and estimated the Hg:OC ratio of pan-Arctic organic and mineral soils to be 0.19 μg g^{-1} and 0.63 μg g^{-1}, respectively. They notably quoted a study by Schuster et al.[51], who reported a Hg:OC ratio of 1.6 ± 1.9 ug g^{-1} for Alaskan soil that they have combined with their own measurements. The Hg:OC ratio in the Mackenzie River, which is the largest Arctic river in terms of sediment discharge[51], is also on the order of 0.6 $\mu g_{Hg}\ g_{OC}^{-1}$ [52–54]. In comparison, the terrigenous endmember Hg:OC ratio in AO sediments is considerably above those values: 6.3 (±0.9) $\mu g_{Hg}\ g_{OC}^{-1}$ on the NAAM, and 11.2 $\mu g_{Hg}\ g_{OC}^{-1}$ in the deep central AO basins. The higher Hg:OC ratios in bottom sediment than in the source material is likely due to regenerative scavenging[15], a process that allows Hg associated with organic particles sinking in oxygenated water columns to be preferentially retained relative to carbon during remineralization[14,55] (Fig. 5). As a result of this process, the Hg:OC ratio in settling particles increases with depth in the water column[14,15,56], so that sediments from marine basins tend to have greater Hg:OC ratios than sediments from shallow coastal zones. On the Arctic continental margin, about 94% of marine OC is remineralized before it reaches the sediments, and this proportion is even greater in the deep central AO[17]. In comparison, about 35% of the terrigenous OC degrades in the water column[17,57]. There is greater remineralization of OC in water column and, consequently, higher Hg:OC ratios in the central basins than on the continental margin, because of the greater transit time.

The data presented here demonstrate that sedimentary Hg concentrations vary by more than an order of magnitude in Arctic Ocean sediments, decrease with depth below the sediment–water interface, parallel the distribution of organic carbon, and covary negatively with increasing $\delta^{13}C$ values. Further, our results reveal that remineralization of OC during its transit to the sediments increases the Hg:OC ratio, while the same processes in suboxic sediment causes this ratio to remain stable with depth in the cores, possibly because Hg is released from the sediments through bacterial methylation and subsequent reductive demethylation (Fig. 5). Although anthropogenic activities have resulted in meaningful Hg contamination in the AO[1,4], our results show that, once Hg reaches this ocean, its distribution is predominantly determined by the cycling of carbon. Unlike observations in other oceans[11–16] and in small Arctic lakes[58], where algal scavenging is expected to be the dominant carrier of Hg to the sediments, in the AO, terrigenous OC appears to play a more important role. The strong connection between Hg and OC implies that any future modifications in organic carbon pathways, including changes arising from permafrost thaw and increasing coastal erosion and river discharge, could have strong effects on the transport and burial of Hg in this ocean.

Methods

Study area

The cores analyzed for this study are from sub-regions of the NAAM where the water depth, primary production, and proportions of terrestrial and marine OC in the sediments exhibit pronounced differences. Our spatial coverage encompasses the North Bering and Chukchi Seas, the Barrow Canyon, the Beaufort Sea margin, the Canadian Archipelago and Lancaster Sound, and the Davis Strait in Southern Baffin Bay (Fig. 1). The Bering and Chukchi Seas receive nutrient-rich Pacific water and are highly productive environments, where the proportion of marine OC in the sediment is higher than that of terrestrial OC[43,59]. At the eastern edge of the Chukchi Sea, the Barrow Canyon includes a regional hotspot of high productivity in its upper portion[59] and accumulates bottom sediments with a high concentration of terrestrial OC[29]. Primary production in the Beaufort Sea is as much as five

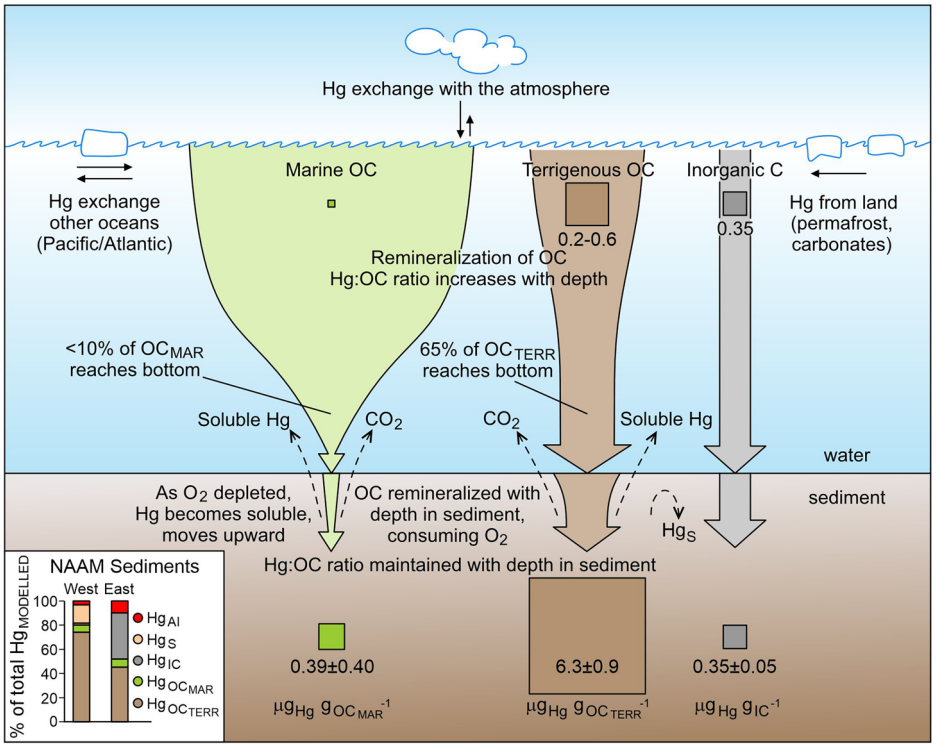

Fig. 5 | Schematic showing how carbon dynamics affect mercury (Hg) delivery to and burial in North American Arctic Margin (NAAM) sediments. Mercury is associated with both marine (OC_{MAR}) and terrigenous (OC_{TERR}) organic carbon. During the transit of particulate organic carbon (OC) through the water column, ~94% of OC_{MAR} and ~35% of OC_{TERR} is remineralized before reaching NAAM sediments. The Hg:OC ratio increases with depth in the water column and during horizontal transport, but remains constant with depth in sediment in most areas. Within the sediment, as OC is remineralized, O_2 is consumed, and Hg is reduced. Most of the soluble, reduced Hg migrates out of the sediment. In shallow, highly productive areas, some of the soluble Hg is recaptured to the solid phase through reactions with authigenic sulphide (Hg_S). OC_{TERR} dominates Hg delivery to the sediments (Hg_{OCTERR}) in the western NAAM, whereas the inorganic carbon contribution (Hg_{IC}) is about equivalent to that from OC_{TERR} at many eastern sites. By comparison, the deposition to the sediments of the Hg associated with OC_{MAR} (Hg_{OCMAR}) and aluminosilicates (Hg_{Al}) are relatively small. Numbers associated with the green, brown, and grey squares in the sediments and in the upper part of the water column represent the content of Hg (μg g^{-1}) in OC_{MAR}, OC_{TERR}, and IC, respectively.

times lower than that of the Chukchi Sea[60,61]. A large amount of terrestrial OC from the Mackenzie River is deposited in this region[24,44]. Further to the East, the Canadian Arctic Archipelago and Lancaster Sound, which together form a complex shelf consisting of multiple channels, and the Davis Strait at the southern entrance of Baffin Bay, are also characterized by much lower rates of biological productivity[62–64] than that of the Chukchi Sea, although autochthonous OC predominates in the sediments[24].

Sampling

As part of the Canadian research program of the International Polar Year, sediment box-cores were collected in the NAAM, from the Canadian Coast Guard Ships (CCGS) *Sir Wilfrid Laurier* and *Louis S. St-Laurent* in 2007 and 2008, respectively[65]. The geographical coordinates of the sampling locations and water depth at each site are reported in Supplementary Table 1. Each core was sub-sampled on board in 0.5-cm intervals for the first 2 cm, 1-cm intervals from 2 to 10 cm depth, and then in progressively thicker layers of 2 and 3 cm down to the bottom of the cores, to a maximum depth of 45 cm. The outermost 2-3 cm of the 600 cm^2 sediment layers in contact with the core liner was discarded, and the sediment samples were stored in double plastic bags and kept frozen for subsequent analyses.

Analysis

The concentration of Hg in freeze-dried sediment samples was determined by gold amalgamation-atomic absorption spectroscopy, using a semi-automatic mercury analyzer (Milestone, DMA-80) and the US EPA standard protocol No. 7473 as a guide. The analytical reproducibility, expressed as a coefficient of variation for replicate analyses ($n = 16$) of the reference sediments MESS-3 from the National Research Council of Canada, was 7.5%. The accuracy (3.8%) was within the range of the certified Hg concentration of the reference material (91 ± 9 ng g^{-1}). For a 100-mg sediment aliquot the detection limit was ca. 1 ng g^{-1}. We report the Hg concentrations on a dry weight basis, after correction for the salt content of the sediment approximated from the measured porosity of each sample and the salinity of the bottom water (~34 on the Practical Salinity Scale). Our cores from NAAM had also been previously analyzed for other elements and isotopes through proven methodologies. Measurements of OC were performed by high temperature combustion of pre-acidified samples, using an NC2500 Thermo Quest Elemental Analyzer, and OC isotopes ($\delta^{13}C$) by high temperature combustion, followed by isotope ratio mass spectrometry using a Carlo Erba 1500 Elemental Analyzer coupled to a ThermoQuest Delta Plus XP Mass Spectrometer[24]. Iron associated with poorly and well-crystallized oxyhydroxides (Fe_{OX}), was determined through extraction with a sodium dithionite solution at pH ~4.7 and ICP-OES measurements[28]. Reduced sulphur (S_{RED}), defined as the total sulphur contained in authigenic iron monosulfide (FeS) and pyrite (FeS_2), was also operationally determined through successive leaching of sediment samples with HCl and Cr(II) solutions and subsequent colorimetric analysis[29]. The occurrence of S_{RED} in the sedimentary column indicates an anoxic condition under which sulphate reduction has been an active reaction.

Sediment geochronology

The sedimentation rates at the coring sites were previously determined through the modeling of the vertical profiles in the sediments of the unsupported ^{210}Pb activity, assuming a surface mixed layer overlying a subsurface sediment layer in which mixing is negligible[26]. The sediment accumulation rates thus estimated for 18 of the cores range from 0.05 to 0.24 cm yr^{-1} (see Supplementary Table 1), with surface mixed layer depths of 0–30 cm. Due to biomixing, the accumulation rates cannot be translated into precise sediment ages at specific depths, but they indicate that a 10-cm-thick layer represents on average 106 ± 42 years of sediment accumulation. Considering that our cores were collected in 2007 and 2008, the uppermost 10 cm of the sediments in the NAAM was deposited during the period of massive anthropogenic Hg emissions into northern hemisphere[30].

Hg associated with IC

Literature data on Hg concentrations in natural carbonates are scarce and relatively old. They are also highly variable, with apparently the lowest levels in biogenic calcareous materials (<10ng g^{-1})[66,67] and the highest levels (>100 ng g^{-1}) in rocks containing carbonaceous fragments[68,69]. Relying on the 1:1 relationship between IC and Ca, or between IC and Ca + Mg, we previously inferred that $CaCO_3$ minerals (i.e., calcite and aragonite) and dolomite (i.e., $CaMg(CO_3)_2$)

were responsible for the sedimentary IC distribution in NAAM sediments[24]. In addition, based on the highly depleted ^{14}C composition of IC in the sediments, we concluded, in agreement with other observations on the composition of the exposed bedrock in the Canadian Archipelago and terrestrial glacial sediments[25,70], that these minerals derive for the most part from detrital sources, not from the production of biogenic calcite or aragonite. Based on this knowledge, we have speculated that the concentration of Hg associated with IC in NAAM sediments can be obtained from the average (±SE) Hg concentration (42 ± 12 ng g^{-1}) reported for Paleozoic shales sampled across the eastern seaboard of Canada[46]. Assuming that these samples comprise pure calcite, their characteristic Hg:IC ratio would therefore be on the order of 0.35 ± 0.05 $\mu g_{Hg}\ g_{IC}^{-1}$. Note that the Hg content in eastern Canada shales is within the range of values characterizing calcareous sedimentary rocks in a variety of environments (4–220 ng g^{-1}), as summarized in Semkin et al.[47]

Hg associated with aluminosilicates

Hg is one of the most poorly constrained elements in the Earth's crust, with reported concentrations varying by an order of magnitude[48,71]. This is likely due to analytical challenges and potential contamination or loss during sample preparation. Because Hg is heterogeneously distributed in the igneous rock, the accuracy of the analyses may also be affected by the size of the sample aliquots[48]. Here, we assume that the aluminosilicate component of NAAM sediments is characterized by a Hg:Al ratio of approximately 30 ± 6 (SE) $ng_{Hg}\ g_{Al}^{-1}$. This value was derived from the average Hg concentration (i.e., 2.3 ± 0.4 (SE) $ng_{Hg}\ g_{SED}^{-1}$, $n = 12$) obtained by Canil et al.[48] for the analysis of large sample aliquots (>30 mg) of Bonanza Arc crust in British Columbia, Canada, previously analyzed for Al[72]. Note that such a low Hg level in crustal material is close to our measured Hg concentrations (<5 $ng_{Hg}\ g_{SED}^{-1}$) at the bottom of cores DS1, DS2, and DS5 from Davis Strait, whose OC concentrations are extremely low (<2 mg g^{-1}).

Hg:OC endmember ratios in NAAM sediments

The fractional contributions of OC_{TERR} (F_{TERR}) and OC_{MAR} (F_{MAR}) in the sediments were first estimated using carbon isotope data, assuming a simple two-component mixing model[73] described by Eq. (1) and Eq. (2):

$$F_{TERR} + F_{MAR} = 1 \quad (1)$$

$$\delta^{13}C_{MEASURED} = F_{MAR} \times \delta^{13}C_{MAR} + F_{TERR} \times \delta^{13}C_{TERR} \quad (2)$$

where $\delta^{13}C_{MEASURED}$ is the measured isotopic composition in the samples, and $\delta^{13}C_{TERR}$ and $\delta^{13}C_{MAR}$ are the isotopic signature endmembers of OC_{TERR} ($\delta^{13}C_{TERR}$ = −26.5‰) and OC_{MAR} ($\delta^{13}C_{MAR}$ = −19.5‰) characterizing the area of study[37–39]. We then assume that Hg associated with inorganic carbon (Hg_{IC}) and aluminosilicates (Hg_{Al}) are obtained based on Eq. (3) and Eq. (4):

$$H_{gIC} = IC_M \times H_g{:}\,IC \quad (3)$$

$$H_{gAl} = Al_M \times H_g{:}\,Al \quad (4)$$

where IC_M and Al_M are the measured IC and Al concentrations, respectively, and Hg:IC (0.35 $\mu g_{Hg}\ g_{IC}^{-1}$) and Hg:Al (30 $ng_{Hg}\ g_{Al}^{-1}$) are the reference ratios characterizing the carbonate components of the sediments and the aluminosilicates (see above). Furthermore, we consider that Hg bonded to sulphides (Hg_S) is negligible except in sediments of Bering and Chukchi Seas where it corresponds to the difference between the positive intercept at OC = 0 of the Hg–OC relationship (16.5 ± 2.3 ng g^{-1}; Supplementary Table 3) and the other forms of inorganic Hg (i.e., Hg_{IC} and Hg_{Al}). Lastly, after having subtracted Hg_{Al}, Hg_{IC} and Hg_S from the measured Hg concentration to determine the Hg:OC ratio free of inorganic Hg, the significant linear regression equation ($p < 0.001$) between this ratio and F_{TERR} (Fig. 4a) was solved for $F_{TERR} = 0$ and $F_{TERR} = 1$ to calculate the Hg:OC endmember ratios of OC_{MAR} and OC_{TERR}, respectively.

Hg:OC endmember ratios in basin sediments

Stable carbon isotope data ($\delta^{13}C$) are not an ideal indicator of carbon sources in central AO basins due to the highly variable carbon isotope composition of phytoplankton[45]. However, using equations deduced for estimating (paleo-) productivity from sediment data, Stein et al.[49] concluded that only 5-20% of the organic matter in central AO sediments is from marine origin, i.e., 80-95% is from terrigenous origin. Assuming that OC_{MAR} and OC_{TERR} represents 20% and 80% of measured OC concentration, respectively, and that the amount of Hg associated with sulphide species is negligible, the Hg:OC endmembers ratios for OC_{MAR} ($Hg{:}OC_{MAR}$) and OC_{TERR} ($Hg{:}OC_{TERR}$) can be inferred by finding the values of these ratios that result in simulated Hg concentrations ($Hg_{MODELLED}$) that best predict the measured Hg concentrations in the samples according to Eq. (5):

$$Hg_{MODELLED} = 0.2\,OC_M \times Hg{:}\,OC_{MAR} + 0.8OC_M \times Hg{:}\,OC_{TERR} + IC_M \times Hg{:}\,IC + Al_M \times Hg{:}\,Al \quad (5)$$

where OC_M, IC_M and Al_M are the measured concentrations of OC, IC and Al, respectively, and Hg:IC and Hg:Al are the same endmember ratios as those characterizing inorganic carbon and aluminosilicates in NAAM sediments.

Statistical assessment

Standard errors (SE) of the intercepts at OC = 0 of the regional linear regressions between Hg and OC in Fig. 3, and of the intercepts at $F_{TERR} = 0$ and $F_{TERR} = 1$ of the linear fit between the stable isotope composition of OC ($\delta^{13}C$) and the fraction of OC from terrigenous source (F_{TERR}) in Fig. 4 were calculated with the statistical function of Excel:

$$SE(b) = \sqrt{(\Sigma(y_i - \hat{y}_i)^2/(n-2) \times [1/n + (\bar{x})^2/\Sigma(x_i - \bar{x})^2])} \quad (6)$$

where b is the intercept, n is the number of observations, $\bar{x}$ is the mean value of x_i, x_i is the individual value, y_i is the observed value, and $\hat{y}_i$ is the predicted value. The results are reported as confidence intervals (CI) corresponding to a significance level of $p = 0.01$.

Data availability

All data generated for this study are included in this published article and its Supplementary Data file. The data are also deposited in the Institute of Ocean Sciences Data Archive: https://www.waterproperties.ca/osd_data_archive/Sediment_Core_Data/NAAM-BASIN-CORES/.

Received: 21 May 2025; Accepted: 20 November 2025;
Published online: 24 December 2025

References

1. AMAP. Assessment 2021: Mercury in the Arctic. Arctic Monitoring and Assessment Programme (AMAP), Tromsø, Norway. 324 pp (2021).
2. Dietz, R. et al. Current state of knowledge on biological effects from contaminants on Arctic wildlife and fish. *Sci. Tot. Environ.* **696**, 133791 (2019).
3. Wang, F. & Macdonald, R. W. *Socioeconomic, political, and legal ramifications of environmental and biochemical toxicology: the complicated story of mercury*. Chap. 11 in Environmental and Biochemical Toxicology, Concepts, Case Studies and Challenges (eds Gailer J. & Turner R. J.), 287-312 (De Gruyter 2022).
4. Dastoor, A. et al. Arctic mercury cycling. *Nat. Rev. Earth Environ.*, **3**, 270–286 (2022).
5. Tesăn Onrubia, J. A. et al. Mercury export flux in the Arctic Ocean estimated from $^{234}Th/^{238}U$ disequilibria. *ACS Earth Space Chem.* **4**, 795–801 (2020).

6. Gleason, J. D. et al. Sources and cycling of mercury in the paleo Arctic Ocean from Hg stable isotope variations in Eocene and Quaternary sediments. *Geochim. Cosmochim. Acta* **197**, 245–262 (2017).
7. Štrok, M., Baya, P. A., Dietrich, D., Dimock, B. & Hintelmann, H. Mercury speciation and mercury stable composition in sediments from Canadian Arctic Archipelago. *Sci. Tot. Environ.* **671**, 655–665 (2019).
8. Kim, D. V. et al. Mercury geochemistry of marine sediments from the eastern Laptev Sea: The spatial distribution, levels, and contamination assessment. *Mar. Pollut. Bul.* **187**, 114576 (2023).
9. Aksentov, K. I. et al. Assessment of mercury levels in modern sediments of the East Siberian Sea. *Mar. Pollut. Bull.* **168**, 112426 (2021).
10. Gobeil, C., Macdonald, R. W. & Smith, J. N. Mercury profiles in sediments of the Arctic Ocean Basins. *Environ. Sci. Technol.* **33**, 4194–4198 (1999).
11. Mason, R. P., Fitzgerald, W. F. & Morel, F. M. M. The biogeochemical cycling of elemental mercury: anthropogenic influences. *Geochim. Cosmochim. Acta* **58**, 3191–3198 (1994).
12. Sunderland, E. M. & Mason, R. P. Human impacts on open ocean mercury concentrations. *Glob. Biogeochem. Cycles* **21**, GB4022 (2007).
13. Gehrke, G. E., Blum, J. D. & Meyers, P. A. The geochemical behavior and isotopic composition of Hg in a mid-Pleistocene western Mediterranean sapropel. *Geochim. Cosmochim. Acta* **73**, 1651–1665 (2009).
14. Munson, K. M., Lamborg, C. H., Swarr, G. J. & Saito, M. A. Mercury species concentrations and fluxes in the Central Tropical Pacific Ocean. *Glob. Biogeochem. Cycles* **29**, 656–676 (2015).
15. Lamborg, C. H., Hammerschmidt, C. R. & Bowman, K. L. 2016 An examination of the role of particles in oceanic mercury cycling. *Philos. Trans. R. Soc. A.* **374**, 20150297 (2016).
16. Zaferani, S., Pérez-Rodriguez, M. & Biester, H. Diatom ooze—A large marine mercury sink. *Science* **361**, 797–800 (2018).
17. Stein, R. & Macdonald, R. W. Organic carbon budget: Arctic Ocean vs. global ocean. Chap. 8 in *The Organic Carbon Cycle in the Arctic* Ocean (eds Stein, R. & Macdonald, R. W.), 315-322 (Springer 2004).
18. Martens, J., Wild, B., Semiletov, I., Dudarev, O. V. & Gustafsson, Ö. Circum-Arctic release of terrestrial carbon varies between regions and sources. *Nat. Commun.* **13**, 5858 (2022).
19. Campeau, A. et al. Sources of riverine mercury across the Mackenzie River Basin: inferences from a combined Hg–C isotopes and optical properties approach. *Sci. Total Environ.* **806**, 150808 (2022).
20. Zhang, Y. et al. Biogeochemical drivers of the fate of riverine mercury discharged to the global and Arctic oceans. *Glob. Biogeochem. Cycles* **29**, 854–864 (2015).
21. Dastoor, A. P. & Durnford, D. A. Arctic Ocean: Is it a sink or a source of atmospheric mercury?. *Environ. Sci. Technol.* **48**, 1707–1717 (2014).
22. Kirk, J. L. et al. Mercury in Arctic marine ecosystems: Sources, pathways and exposure. *Environ. Res.* **119**, 64–87 (2012).
23. Coquery, M., Cossa, D. & Martin, J. M. The distribution of dissolved and particulate mercury in three Siberian estuaries and adjacent Arctic coastal waters. *Water Air Soil Pollut.* **80**, 653–664 (1995).
24. Goñi, M. A. et al. Distribution and sources of organic matter in surface marine sediments across the North American Arctic margin. *J. Geophys. Res. Oceans* **118**, 4017–4035 (2013).
25. Hamilton, P. B., Gajewski, K., Atkinson, D. E. & Lean, R. S. Physical and chemical limnilogy of 204 lakes from the Canadian Arctic Archipelago. *Hydrobiologia* **457**, 133–148 (2001).
26. Kuzyk, Z. A., Gobeil, C. & Macdonald, R. W. ^{210}Pb and ^{137}Cs in margin sediments of the Arctic Ocean: controls on boundary scavenging. *Glob. Biogeochem.* **27**, 422–439 (2013).
27. Berner, R. A. Sedimentary pyrite formation: An update. *Geochim. Cosmochim. Acta* **48**, 605–615 (1984).
28. Macdonald, R. W. & Gobeil, C. Manganese sources and sinks in the Arctic Ocean with reference to periodic enrichments in basin sediments. *Aquat. Geochem.* **18**, 565–591 (2012).
29. Kuzyk, Z. Z. A., Gobeil, C., Goñi, M. A. & Macdonald, R. W. Early diagenesis and trace element accumulation in North American Arctic margin sediments. *Geochim. Cosmochim. Acta* **203**, 175–200 (2017).
30. Streets, D. G. et al. Total mercury released to the environment by human activities. *Environ. Sci. Technol.* **51**, 5969–5977 (2017).
31. Huerta-Diaz, M. A. & Morse, J. W. Pyritization of trace metals in anoxic marine sediments. *Geochim. Cosmochim. Acta* **56**, 2681–2702 (1992).
32. Manceau, A. et al. Formation of mercury sulfide from Hg(II)–thiolate complexes in natural organic matter. *Environ. Sci. Technol.* **49**, 9787–9796 (2015).
33. Hammerschmidt, C. R., Fitzgerald, W. F., Lamborg, C. H., Balcom, P. H. & Visscher, P. T. Biogeochemistry of methylmercury in sediments of Long Island Sound. *Mar. Chem.* **90**, 31–52 (2004).
34. Hammerschmidt, C. R. & Fitzgerald, W. F. Geochemical controls on the production and distribution of methylmercury in near-shore marine sediments. *Environ. Sci. Technol.* **38**, 1487–1495 (2004).
35. Jeong, H. Y., Klaue, B., Blum, J. D. & Hayes, K. F. Sorption of mercuric ion by synthetic nanocrystalline Mackinawite (FeS). *Environ. Sci. Technol.* **41**, 7699–7705 (2007).
36. Feyte, S., Gobeil, C., Tessier, A. & Cossa, D. Mercury dynamics in lake sediments. *Geochim. Cosmochim. Acta* **82**, 92–112 (2012).
37. Frieling, J. et al. Effects of redox variability and early diagenesis on marine sedimentary Hg records. *Geochim. Cosmochim. Acta* **351**, 78–95 (2023).
38. Cossa, D., Coquery, M., Gobeil, C. & Martin, J. M. Mercury Fluxes at the Ocean Margins. In: Baeyens, W., Ebinghaus, R., Vasiliev, O. (eds) *Global and Regional Mercury Cycles: Sources, Fluxes and Mass Balances*. NATO ASI Series, 21 (1996). Springer, Dordrecht.
39. Weber, J. H., Evans, R., Jones, S. H. & Hines, M. E. Conversion of mercury(II) into mercury(0), monomethylmercury cation, and dimethylmercury in salt marsh sediment slurries. *Chemosphere* **36**, 1669–1687 (1998).
40. Helmrich, S., Vlassopoulos, D., Alpers, C. N. & O'Day, P. A. Critical review of mercury methylation and methylmercury demethylation rate constants in aquatic sediments for biogeochemical modeling. *Crit. Rev. Environ. Sci. Technol.* **52**, 4353–4378 (2022).
41. Gu, B. et al. Mercury reduction and complexation by natural organic matter in anoxic environments. *Proc. Natl. Acad. Sci.* **108**, 1479–1483 (2011).
42. Kim, J. et al. Mass budget in methylmercury in East Siberian Sea: the importance of sediment sources. *Environ. Sci. Technol.* **54**, 949–957 (2020).
43. Naidu, A. S. et al. Organic carbon isotope ratios (δ^{13}C) of Amerasian continental shelf sediments. *Int. J. Earth Sci.* **89**, 522–532 (2000).
44. Goñi, M. A., Yunker, M. B., Macdonald, R. W. & Eglinton, T. I. Distribution and sources of organic biomarkers in arctic sediments from the Mackenzie River and Beaufort Shelf. *Mar. Chem.* **7**, 23–51 (2000).
45. Schubert, C. J. & Calvert, S. E. Nitrogen and carbon isotopic composition of marine and terrestrial organic matter in Arctic Ocean in sediments: implications for nutrient utilization and organic matter composition. *Deep-Sea Res.* **46**, 789–810 (2001).
46. Cameron, E. M. & Jonasson, I. R. Mercury in Precambrian shales of the Canadian Shield. *Geochim. Cosmochim. Acta* **36**, 985–1005 (1972).
47. Semkin, R. G., Mierle, G. & Neureuther, R. J. Hydrochemistry and mercury cycling in a High Arctic watershed. *Sci. Total Environ.* **342**, 199–221 (2005).
48. Canil, D., Crockford, P. W., Rossin, R. & Telmer, K. Mercury in some arc crustal and mantle peridotites and relevance to the moderately volatile element budget of the Earth. *Chem. Geol.* **396**, 134–142 (2015).

49. Stein, R. et al. The central Arctic Ocean: distribution, sources, variability, and burial of organic carbon. Chap. 7.9 in *The Organic Carbon Cycle in the Arctic Ocean* (eds Stein, R. & Macdonald, R. W.), 295–314 (Springer 2004).
50. Lim, A. G. et al. A revised pan-Arctic permafrost soil Hg pool based on Western Siberian peat Hg and carbon observations. *Biogeosciences* **17**, 3083–3097 (2020).
51. Schuster, P. F. et al. Permafrost stores a globally significant amount of mercury. *Geophys. Res. Lett.* **45**, 1463–1471 (2018).
52. Leitch, D. R. et al. The delivery of mercury to the Beaufort Sea of the Arctic Ocean by the Mackenzie River. *Sci. Total Environ.* **373**, 178–195 (2007).
53. Rachold, V. et al. Modern terrigenous organic carbon input to the Arctic Ocean. Chap. 2 in *The Organic Carbon Cycle in the Arctic Ocean* (eds Stein, R. & Macdonald, R. W.), 33–55 (Springer, 2004).
54. Zolkos, S. et al. Mercury export from Arctic great rivers. *Environ. Sci. Technol.* **54**, 4140–4148 (2020).
55. Qu, Y., Zhong, H., Liu, X., Zhang, W. & Chen, T. Coupling and decoupling between sedimentary mercury and organic carbon preservation in the oxygenated marine environment. *Geochem. Geophys.* **25**, e2023Gc011201 (2024).
56. Cossa, D. et al. Mercury accumulation in the sediment of the Western Mediterranean abyssal plain: A reliable archive of the late Holocene. *Geochim. Cosmochim. Acta* **309**, 1–15 (2021).
57. Ittekkot, V. Global trends in the nature of organic matter in river suspension. *Nature* **322**, 436–438 (1988).
58. Outridge, P. M., Stern, G. A., Hamilton, P. B. & Sanei, H. Algal scavenging of mercury in preindustrial Arctic lakes. *Limnol. Oceanogr.* **64**, 1558–1571 (2019).
59. Naidu, A. S. et al. The continental margin of the North Bering Chukchi Seas: concentrations, sources, fluxes, accumulation and burial rates of organic carbon. Chap. 7.3 in *The Organic Carbon Cycle in the Arctic* Ocean (eds Stein, R. & Macdonald, R.W.), 193-203 (Springer 2004).
60. Grebmeier, J. M., Cooper, L. W., Feder, H. M. & Sirenko, B. I. Ecosystem dynamics of the Pacific-influenced Northern Bering and Chukchi Seas in the Amerasian Arctic. *Prog. Oceanogr.* **71**, 331–361 (2006).
61. Macdonald, R. W., Wong, C. S. & Erickson, P. E. The distribution of nutrients in the southeastern Beaufort Sea: Implications for water circulation and primary production. *J. Geophys. Res.* **92**, 2939–2952 (1987).
62. Sakshaug, E. Primary and secondary production in the Arctic Seas. Chap. 3 in *The organic carbon cycle in the Arctic Ocean* (eds. Stein, R. & Macdonald, R. W.), 57-81 (Springer, 2004)
63. Platt, T., Harrison, W. G., Irwin, B., Horne, E. P. & Gallegos, C. L. Photosynthesis and photodegradation of marine phytoplankton in the Arctic. *Deep-Sea Res. Part A* **29**, 1159–1170 (1982).
64. Jensen, H. M., Pedersen, L., Burmeister, A. & Hansen, B. W. Pelagic primary production during summer along 65 to 72°N off West Greenland. *Pol. Biol.* **21**, 269–278 (1999).
65. Carmack, E. C., McLaughlin, F. A., Vagle, S., Melling, H. & Williams, W. J. Structures and property distributions in the three oceans surrounding Canada in 2007: a basis for a long-term ocean climate monitoring strategy. *Atmos. Ocean* **48**, 211–224 (2010).
66. Meyer, K. W. et al. Biogenic carbonate mercury and marine temperature records reveal global influence of Late Cretaceous Deccan Traps. *Nat. Commun.* **10**, 5356 (2019).
67. Cao, F. et al. A digestion-purging-trapping method for precise stable mercury isotope measurements of natural carbonates. *J. Anal. Spectrom.* **40**, 1373 (2025).
68. Pasquetti, F. et al. Sedimentological, mineralogical and geochemical features of late Quaternary sediment profiles from the southern Tuscany Hg district (Italy): evidence for the presence of pre-industrial mercury and arsenic. *Water* **12**, 1998 (2020).
69. Lieu, J., Rong, Y. & Zhang, S. Mineralogy of Zn-Hg-S and Hg-Se-S series minerals in carbonate-hosted mercury deposits in Western Hunan, South China. *Minerals* **7**, 101 (2017).
70. Andrews, J. T. et al. The surficial geology of the Canadian eastern Arctic and Polar continental shelves. *Cont. Shelf Res.* **11**, 791–819 (1991).
71. Rudnick,R. L. & Gao, S. Composition of the continental crust. In Treatise on Geochemistry, 3 (ed. R. L. Rudnick). Elsevier, pp. 1–64 (2003).
72. Larocque, J. & Canil, D. The role of amphibole in the evolution of arc magmas and crust: the case from the Jurassic Bonanza arc section, Vancouver Island, Canada. *Contrib. Mineral. Petrol.* **159**, 475–492 (2010).
73. Fry, B., Scalan, R. S. & Parker, P. L. Stable carbon isotope evidence for two sources of organic matter in coastal sediments: seagrasses and plankton. *Geochim. Cosmochim. Acta* **41**, 1875–1877 (1977).

Acknowledgements

We gratefully acknowledge the Program for the International Polar Year of the Canadian Government, the Department of Fisheries and Oceans, and the Natural Sciences and Engineering Research Council of Canada for their financial support. We also thank the captains and crews of the Canadian Coast Guard Ships *Sir Wilfrid Laurier* (July 2007) and *Louis S. St- Laurent* (July 2008) and acknowledge S. Jobidon for support in the laboratory, L. Rancourt for research assistance, and P. Kimber for drafting the diagrams.

Author contributions

C.G. conceived and designed this study with our late colleague Robie W. Macdonald and obtained the financial support; C.G. and S.J. interpreted the data, wrote the manuscript, and created the figures. M.A.G. and C.G. supervised and performed the sampling and analytical work. M.A.G., Z.Z.A.K., and D.C. contributed to data interpretation, statistical treatment,s and manuscript revision.

Competing interests

The authors declare no competing interests. Note that Dr. Sophia Johannessen, one of the coauthors, is on the editorial board of Communications Earth & Environment, but was not involved in the editorial review of, nor the decision to publish this article.

Additional information

Supplementary information The online version contains supplementary material available at https://doi.org/10.1038/s43247-025-03058-7.

Correspondence and requests for materials should be addressed to Charles Gobeil.

Peer review information *Communications Earth and Environment* thanks Xiangming Shi, Alyssa Azaroff and Ruoyu Sun for their contribution to the peer review of this work. Primary Handling Editor: Alice Drinkwater. A peer review file is available.